Fabrication of noncollinear antiferromagnetic Mn-Sn thin films and evaluation of their crystal structures and transport properties

著者	Yoon Juyoung
journal or publication title	東北大学電通談話会記録
volume	89
number	2
page range	16-17
year	2021-03-04
URL	http://hdl.handle.net/10097/00130876

修士学位論文要約（令和２年９月）

ノンコリニア反強磁性 Mn-Sn 薄膜の作製と結晶構造・輸送特性の評価

ユン　ジュヨン

指導教員：深見 俊輔

Fabrication of noncollinear antiferromagnetic Mn-Sn thin films and evaluation of their crystal structures and transport properties

Juyoung Yoon

Supervisor: Shunsuke FUKAMI

I study the growth technique of non-collinear antiferromagnetic Mn_3Sn thin films deposited by sputtering with various substrates and underlayers. Relation between their crystal structure and magnetic/transport properties is also investigated. I achieve a formation of epitaxial films with both C-plane and M-plane orientations, whose Kagome lattices are parallel and perpendicular to the plane, respectively. Transverse resistivity originating from the anomalous Hall effect shows different trends reflecting the Kagome lattice orientations of each stack. The established technique and findings offer a platform to study functional devices utilizing unconventional physical properties of non-collinear antiferromagnets with controlled Kagome lattice orientation.

1. Introduction

Non-collinear antiferromagnetic materials with kagome lattice such as $D0_{19}$-Mn_3Sn and Mn_3Ge have attracted increasing attention owing to their large anomalous Hall effect (AHE) originating from non-trivial Berry curvature mediated by the non-collinear spin texture[1,2]. In order to explore the functionalities of these phenomena for device applications, it is of importance to establish technique to grow thin films with a single crystalline phase.

Many physical properties of Mn_3Sn have been revealed in bulk single crystal[1,2]. Meanwhile, few studies on Mn_3Sn thin film have been performed and magneto-transport property of Mn_3Sn film has been investigated only for poly-crystalline samples[3,4]. In this work, I study the growth of epitaxial $D0_{19}$-Mn_3Sn thin films with various crystal orientations. I also measure magneto-transport properties and discuss the relation between crystal orientation and transport properties.

2. Methods

I deposit Mn_3Sn thin films by magnetron sputtering at 400°C on various substrates and underlayers (ULs). The samples are annealed at 500°C for an hour. Crystal structure and transport properties are characterized by X-ray diffraction (XRD) and physical property measurement system, respectively. The transport measurement is performed for Hall-bar devices at room temperature.

3. Analysis of crystal structures

Figure 1(a) shows 2θ-θ XRD spectra for Si sub./Ta(5 nm)/Mn_3Sn(50 nm) and Si sub./Ta(2 nm)/Ru(5 nm)/Mn_3Sn(30 nm) (thickness in nm). For UL = Ta, several weak peaks of Mn_3Sn indicating no preferential orientation are observed. For UL = Ta/Ru, on the other hand, prominent peaks of C-plane oriented Mn_3Sn are observed. However, as the Mn_3Sn thickness increases beyond 50 nm, $(2\bar{2}01)$ peak indicating different orientation appears at $2\theta \simeq 42^{\circ}$ [Fig. 1(b)]. To overcome this issue and form epitaxial films, I use single crystalline MgO substrates. Figure 1(c) shows 2θ-θ spectra for MgO(111) sub./Ru(5 nm)/Mn_3Sn (30 or 80 nm). Only (0002) and (0004) peaks are observed regardless of the thickness, indicating C-plane orientation even for thicker films. I then turn to an M-plane oriented epitaxial Mn_3Sn film. I first use W as an underlayer because of a small lattice mismatch between W and Mn_3Sn. Figure 1(d) shows the 2θ-θ XRD spectra for MgO(110) sub./W (10 nm)/Mn_3Sn (50 nm). In addition to the expected $(1\bar{1}00)$, $(2\bar{2}00)$, $(4\bar{4}00)$ peaks, unexpected peaks are observed at $2\theta \simeq 24^{\circ}$ and 79°, which can be attributed to WMn_2Sn formed through intermixing of W and Mn_3Sn layers. To avoid the formation of this intermixing layer, I insert a thin Ta layer between W and Mn_3Sn. As shown in Fig. 1(e), WMn_2Sn peaks are

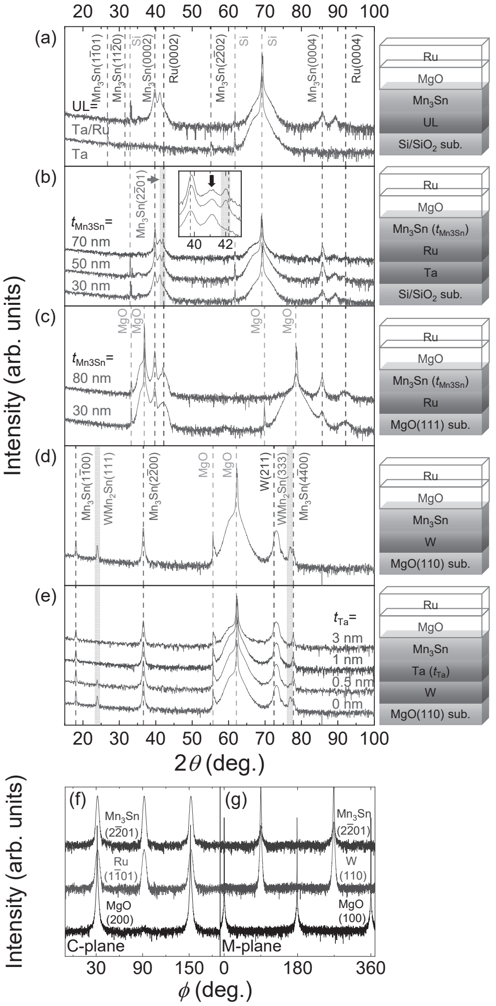

Fig. 1. (a)-(e) XRD spectra of 2θ-θ scans for the stack structures shown on the right. (f), (g) XRD spectra of ϕ-scan for stack structures in Fig. 1 (c) and (e) respectively.

eliminated by the Ta insertion. Both the C-plane and M-plane oriented Mn_3Sn is epitaxial in in-plane orientation too as shown in Fig.1(f), (g).

4. Magneto-transport properties

Figures 2(a)-(d) show Hall resistivity(ρ_{xy}) as a function of out-of-plane magnetic field (H) in poly-crystalline, C-plane dominant poly-crystalline, epitaxial C-plane, and epitaxial M-plane Mn_3Sn thin films, respectively. Clear hysteresis with respect to the out-of-plane field is observed in M-plane-oriented stack [Fig. 2(d)], but not in the C-plane-oriented stack [Fig. 2(c)]. This result can be accouted for by AHE

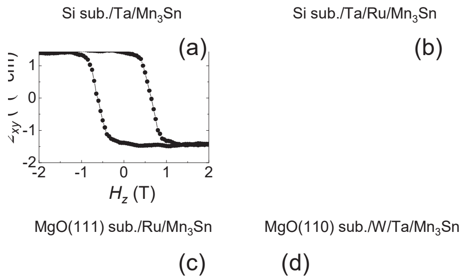

Fig. 2. (a)-(d) ρ_{xy} vs. H for Mn_3Sn thin films deposited with the stack structures above the figures.

induced by Berry curvature arising in the kagome plane. ρ_{xy} of poly-crystalline Mn_3Sn (1.4 μΩcm) [Fig. 2(a)] agrees well with previous studies[3,4]. For stacks of Si sub./Ta/Ru/Mn_3Sn, ρ_{xy} increases with Mn_3Sn thickness [Fig. 2(b)], in consistent with the formation of $Mn_3Sn(2\bar{2}01)$ revealed by XRD.

5. Summary

In summary, I study crystalline structure and transport properties of non-collinear antiferromagnetic Mn_3Sn thin films deposited by sputtering. Crystal orientation of Mn_3Sn is controlled by choosing appropriate substrates and ULs. AHE of Mn_3Sn depending on crystalline orientation is observed, proving anisotropic Berry curvature in non-collinear antiferromagnet. The obtained technique to prepare Mn_3Sn thin film with controlled crystal orientation provide the basis to study the functionalities of non-collinear antiferromagnets[5].

This work is partly supported by JSPS Kakenhi (No. 19H05622 and No. 19J13405).

Reference

1) S. Nakastuji *et al.*, Nature **527**, 212 (2015).
2) A. K. Nayak *et al.*, Sci. Adv. **2**, e1501870 (2016).
3) T. Higo *et al.*, Appl. Phys. Lett. **113**, 202402 (2018).
4) T. Ikeda *et al.*, Appl. Phys. Lett. **113**, 222405 (2018).
5) J. Yoon *et al.*, Appl. Phys. Express **13**, 013001 (2020).